# Structural and folding properties of a lattice prion model

Andrew F. Wind, Josh P. Kemp, Aleksander V. Ermoshkin, and Jeff Z. Y. Chen*
*Department of Physics, University of Waterloo, Waterloo, Ontario, Canada N2L 3G1*
(Received 16 May 2002; published 24 September 2002)

Searching through and conducting Monte Carlo folding simulations on $10^6$ different 27 mer sequences, we have selected a prionlike lattice model whose energy spectrum and folding properties demonstrate characteristic prion behavior. The energetic competition and structural partition between two closely spaced energy minima yield unique kinetic and thermodynamic properties that can be qualitatively compared with experimental results. Folding simulations indicate that the probability of reaching the first excited state from a denatured random conformation is much higher than the probability of reaching the global energy-minimum state.

DOI: 10.1103/PhysRevE.66.031909 PACS number(s): 87.15.−v, 87.14.Ee, 36.20.Ey

## I. INTRODUCTION

A prion protein is a specific type of protein that has two native states rather than one [1]. One of the native states is kinetically favored and behaves similarly to a fast folding protein. The other state, the prion state, is less likely to be adopted naturally but has been implicated as the cause of some rare diseases including bovine spongiform encephalopathy (mad cow disease), Creutzfeld Jakob disease, Kuru, and scrapies. The protein in the prion state is the infectious agent and there is no need for the involvement of nucleic acids such as DNA or RNA in an infection scenario. A prion protein in the prion state acts as a template to convert other proteins, present in the native state, to adopt the prion state. This hypothesis has been overwhelmingly supported by experimental evidence although the actual infection scenarios are still not completely clear [2–6].

In the past few years, lattice models have been widely used to explore the basic folding properties of proteins in general. The current understanding of the general features of protein folding is largely dependent on the recent progress in Monte Carlo (MC) simulations of lattice protein models [7–11]. In this paper, we examine the folding properties and landscape of a general 27 mer lattice model and explore the possibility of finding prionlike protein structures within the framework of a 27 mer model. The general aspects of the 27 mer model are the same as those used by Šali, Shakhnovich, and Karplus [7] and the model has been well studied recently for its relevance in protein folding. In contrast to the approach of Abkevich, Gutin, and Shakhnovich [12], who designed their prion molecules to have specific structural features, we attempt to identify prionlike sequences strictly based on screening an ensemble of sequences ''naturally'' occurring from a sequence generation process. Through a study of each sequence's energy spectrum and lowest-energy structures, 273 sequences out of $10^6$ randomly generated sequences were found to be possible candidates for study. Further analyzing the folding properties of this subset indicates that only a couple of the sequences have prionlike behavior, one of them being analyzed in detail in this paper. The small percentage of prionlike structures generated in our simulations is an indication of the rare occurrence, however, inherent existence, of prion proteins in nature (see Sec. II).

Lattice models have established that a characteristic feature of a proteinlike chain is a funnel-like energy landscape in terms of configurations [13]. This landscape directs the folding of a protein to a single native state. The existence of two competing low-energy states, however, complicates the folding pathways and exhibits special funnel structures. Through an examination of the density of states, especially in the low-energy regime, we are able to observe the openness of the folding funnel and the connectivity between the low-energy states and possible intermediate states (Sec. III C). The density of states can then be compared with the kinetic folding simulations performed to demonstrate the kinetic folding trajectories (Sec. III A).

## II. MODEL AND THE SELECTION OF THE PRIONLIKE SEQUENCES

The 27 mer lattice model has been extensively studied in literature. In order to compare our results with the previous 27 mer studies, we have generated the protein sequences following the procedure described by Šali, Shakhnovich, and Karplus [8]. Initially, a set of contact potential energies is selected randomly from a Gaussian distribution which is centered at $-2\epsilon$ and has a standard deviation of $\epsilon$. Here, $\epsilon$ is a basic energy unit that can be absorbed into the definition of a reduced temperature, $\overline{T}=k_BT/\epsilon$. As a cubic conformation is the most compact arrangement and contains the maximum number of contacts, the lowest-energy conformations are likely to be cubic, although not guaranteed. In a ''normal'' protein model, the ground state is deemed to be the native state because it is probably the lowest *free-energy* configuration as well.

We restrict our search for prionlike candidates by imposing the following conditions.

(a) The two lowest-energy cubic states, a ground state and an excited state, must have similar energies. This condition originates from experimental evidence that suggests that the two conformations of a prion might be only marginally different [4].

*Author to whom correspondence should be addressed.

 

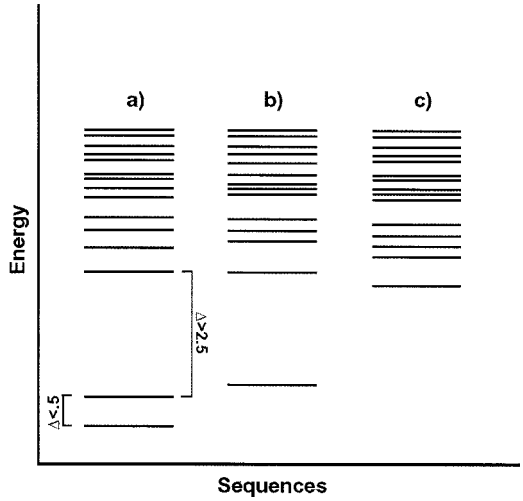


FIG. 1. (a) The energy spectrum of a prionlike sequence. (b) The energy spectrum of a good folding sequence. Note the large gap between the lowest and second lowest-energy states. (c) The energy spectrum of a sequence with glassy characteristics.

(b) These two lowest-energy compact states must be significantly separated by a large gap from the energy spectrum of the remaining compact states. This restriction comes from previous protein folding studies which show that proteinlike sequences have large energy gaps separating a native state from other compact configurations.

(c) The ground state and excited state must have significantly different structures. This is a requirement that prevents the occurrence of a small energy difference due to a minor structural variation.

(d) The sequence has to be a *good folder* with respect to one of the two lowest-energy states. We use the definition in Ref. [8], which states that a good folder reaches its native state 40% of the time in a simulation five times longer than the mean first passage time (MFPT).

(e) A large free energy barrier must kinetically separate the ground and excited states.

These selection rules are implemented in our study as follows. First, sequences are generated, each corresponding to a random contact energy matrix. The energies of compact configurations of a given sequence are determined through exact enumeration to produce an energy spectrum of the compact states. Sequences with an energy spectrum similar to the one shown in Fig. 1(a) are considered possible prion candidates. The desired spectrum is based on conditions (a) and (b), and is constructed by accepting sequences whose two lowest energies are separated by less than $0.5\epsilon$ and have a gap of greater than $2.5\epsilon$ between the second and third lowest energies. The sequences that meet these two criteria are then examined in terms of structural differences between the two lowest-energy states, under condition (c). The structural similarity is measured by determining the number of monomers situated in the same position of the cube. To identify these monomers, the cubic structures are studied with the same orientation. If structures have less than three monomers in the same lattice positions, the structures are considered sufficiently different.

To determine the folding ability of these chosen sequences, MC folding simulations were run on a multiprocessor computation environment. The Monte Carlo folding simulations were conducted at different temperatures for different sequences. The temperature was selected to warrant [8]

$$\sum_{i=\mathrm{CSA}} \left( \frac{e^{-E_i/k_BT}}{\sum_{i=\mathrm{CSA}} e^{-E_i/k_BT}} \right)^2 = 0.2, \tag{1}$$

where CSA represents all compact self-avoiding states on cubic arrangements. Here we have generated all 103 346 cubic configurations through an exhaustive enumeration procedure. This temperature is believed to be a good estimate for the ideal temperature at which the folding simulations should be conducted.

A prion candidate was then folded 50 times, each consisting of $1\times10^9$ Monte Carlo steps, where one Monte Carlo step is defined as one attempted local move as described in Ref. [7]. The simulation results determine whether conditions (d) and (e) are satisfied by the selected sequence. To facilitate the discussion, the ground state will be referred to as I and the excited-energy state as II. A sequence is considered a good folder if either state I or II fits the conditions given above. This good folding state, whether it is the ground state (I) or the excited state (II), is called the native state. Finally, we are only interested in those sequences that are kinetically partitioned by a large free energy barrier, as stated in (e). Therefore, the other state, of I or II, should be rarely visited in folding events when compared with the frequency of visits to the native state and will be termed the prion state.

Out of the $10^6$ sequences randomly generated, 0.03% met the required conditions on the energy spectrum and structural differences. The majority of these sequences were good folders but could not be qualified as a prion model and therefore were not used for further study. Among the final prototypes with prionlike characteristics, two sequences were selected for in-depth study because they are prionlike. Both sequences were given considerably more computational effort and have been folded for an additional 2000 Monte Carlo runs each. The study of one of them will be discussed in detail below.

## III. FOLDING AND THERMODYNAMIC PROPERTIES

### A. Kinetic folding of the prionlike sequence

The model corresponding to the selected sequence demonstrates the characteristic properties of a prion protein, which have been observed experimentally. Energetically the native ($PrP^C$) state is only marginally less stable than the infectious ($PrP^{Sc}$) prion state [4]. However, under normal biological conditions, the native $PrP^C$ state is the kinetically favored state in the folding pathway.

A typical MC kinetic simulation started with an initial configuration selected from a self-avoiding random walk. The time-dependent trajectory of 2000 MC simulations, each containing $1\times10^9$ MC steps, has been examined. For this sequence, 72.1% of the time the polymer folds into state II

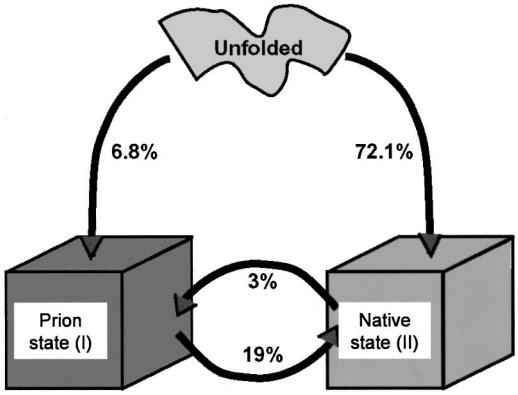


FIG. 2. Diagram displaying the successful folding percentages between the various states for the prionlike sequence studied in this paper. The remainder of the folding events not shown are unsuccessful folding events where the target configurations were not reached. The results beginning in the unfolded states are based on 2000 simulations, while the transition results between the two native states are obtained from 100 simulations each. Each simulation is $1\times10^9$ Monte Carlo steps.

(the first excited-energy state), without the immediate involvement of state I. Hence the first excited state is the native state of the sequence and the ground state is the prion state. In addition, 6.8% of the folding trajectories reached I without passing through state II. The remainder of the simulation events reach a variety of higher-energy local minima, in which we have no interest. Due to the limited simulation time, these local minima never had a chance to further refold into the low-energy states.

To further explore the folding properties, an additional 200 MC simulations of the same time length were conducted. Attention is now paid to the transition between the two lowest-energy states. The first 100 simulations started from the native state, II, and were allowed to unfold and refold, possibly into state I, the prion state. Only 3% of the simulations reached the prion state in the simulation time allowed. The next 100 simulations were designed to handle the reverse process, where state I was designated as the initial starting configuration and the polymer was allowed to unfold and refold. In the reverse process, 19% of the simulations reached the native state starting from the prion state within the given simulation time. These folding and transition results are depicted in Fig. 2. Note that the transition time is much longer than the MFPT as presented in Table I.

Though we are dealing with a very simple 27 mer model, it demonstrates kinetic properties that bear amazing resemblance to a prion. The native state, which has a higher energy, is a fast-folding structure and is kinetically more accessible than the other states. The prion state has a lower energy very close to the native state and is partitioned sufficiently ''far'' from the general folding landscape. This kinetic partitioning is demonstrated by the small percentage of crossovers from the native state to the prion state. There exist two separate folding funnel pathways similar to a recent concept suggested by Abkevich, Gutin, and Shakhnovich [12]. The pathways are connected through energy states that are much higher than those immediately above these two states. The single funnel from the connection of the two pathways down to native state is more kinetically direct than the funnel to the prion state. We infer this from the fact that the percentage of crossover events is not symmetric, and that there is a higher probability of moving from the prion state to the native state than the reverse process.

TABLE I. The first passage times for the prionlike model. Shown is the number of folded events taken to calculate each average, total number of events simulated, followed by the mean first passage time. Here *U* represents an unfolded state, and the number in parentheses represents the standard variations.

| Path | No. of folded events | No. of attempts | Time (MC steps) |
|---|---|---|---|
| $U\rightarrow$I | 136 | 2000 | $3.0(3)\times10^8$ |
| $U\rightarrow$II | 1442 | 2000 | $3.24(7)\times10^8$ |
| I$\rightarrow$II | 19 | 100 | $6.0(6)\times10^8$ |
| I$\rightarrow$I | 3 | 100 | $6.2(7)\times10^8$ |

This is in contrast with the theory of an intermediate state model where a protein folds first to a stable intermediate state and then to its ground state. If such an intermediate state model were applicable to prion pathways, we would expect to observe the percentages of crossover in reverse order. The existence of the intermediate folding scenario was also questioned both in lattice models [9] and in experiments [14] where fast-folding proteins do not fold with the aid of intermediates.

### B. Order parameter

The structural overlapping parameter provides a measurement of the structural similarity between the configuration under examination and the native configuration. It is defined as the ratio of the number of common bonds between the two conformations over the total number of bonds in the reference conformation. Taking the ground state as the reference, we consider

$$Q^{[\mathrm{I}]}(i)=\frac{N^{[\mathrm{I}]}_{\mathrm{common}}(i)}{N^{[\mathrm{I}]}_{\mathrm{total}}}, \tag{2}$$

where I represents the ground state and $i$ represents the current conformation. $N^{[\mathrm{I}]}_{\mathrm{total}}$ is the total number of bonds present in state I. Thus, $N^{[\mathrm{I}]}_{\mathrm{total}}$ reaches a maximum value of 28 for a compact cubic structure such as the ground state. The structural overlapping parameter is therefore bounded between zero and unity. If the reference conformation is a compact state, a value of unity identifies the current conformation as identical to the reference conformation since all possible bonds are accounted for.

The difference between two measurements taken with respect to separate references can be used to consider the structural distance of a structure from two states. In the case of prions, we are interested in a single order parameter that represents the distance between the native and prion states. Therefore, in our study we define an order parameter $x$,

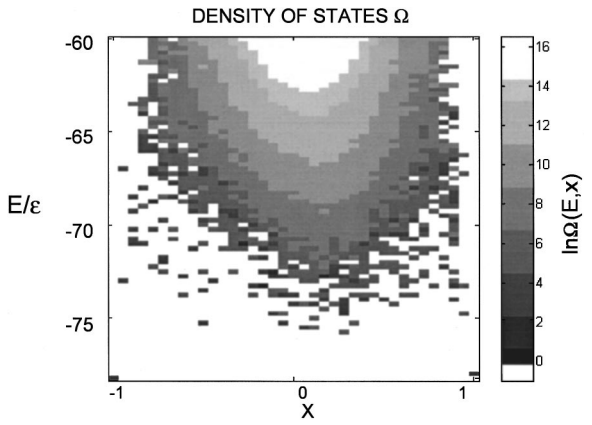


FIG. 3. The density of states as a function of $E$ and $x$. Notice that the density of states is leaning toward the native state to the right.

$$x(i)=\frac{Q^{[\mathrm{II}]}(i)-Q^{[\mathrm{I}]}(i)}{1-Q^{[\mathrm{I}]}(\mathrm{II})/Q^{[\mathrm{I}]}(\mathrm{I})}, \tag{3}$$

where the denominator serves to normalize the parameter between $-1$ and 1. This is performed in cases I and II sharing common bonds as they do in our study sequences. Hence we have $x=-1$ for the ground state (prion state) and $x=1$ for the excited state (native state).

### C. Density of states

As an effective measurement of the degrees of freedom that are available to various given energy levels, we consider a calculation of the density of states of the system as a function of $E$ and the order parameter $x$. Such a study determines the energy landscape, at least thermodynamically, in terms of a function of the order parameter $x$.

Our calculation is based on an implementation of the multicanonical Monte Carlo technique that promises to sample every energy evenly and represents a one-dimensional random walk in the energy space [15]. The density of states is directly calculated from a histogram of the number of states visited during the simulation by multiplying the distribution with the inverse of the weight factor. Rescaling has been performed to acknowledge the fact that there is a unique ground state and therefore it should correspond to a single state.

The density of states directly shows several key features of the selected prionlike sequence as displayed in Fig. 3. We observe from this plot that there are more states accessible to the right side leading to the native structure than to the left, leading to the prion state. The density of the entire map is leaning towards $x=1$. By examining the folding trajectory we found that almost all energy states on the right are directly related to the native state in the folding pathway. Hence, these states provide a funnel-like landscape.

In contrast, the existence of apparent intermediate states on the $x<0$ side near $x=0$ is somewhat misleading in Fig. 3. By following the folding trajectories of the MC simulations, we found that the immediate state that the model must go through kinetically to fold into the prion state at the low left corner is the state at $x\approx 0.95$ and $E\approx -73$. This makes the folding to the prion state more difficult, since the states in the vicinity of this ''prerequisite'' are more sparse than the states that lead to the native structure on the right hand side.

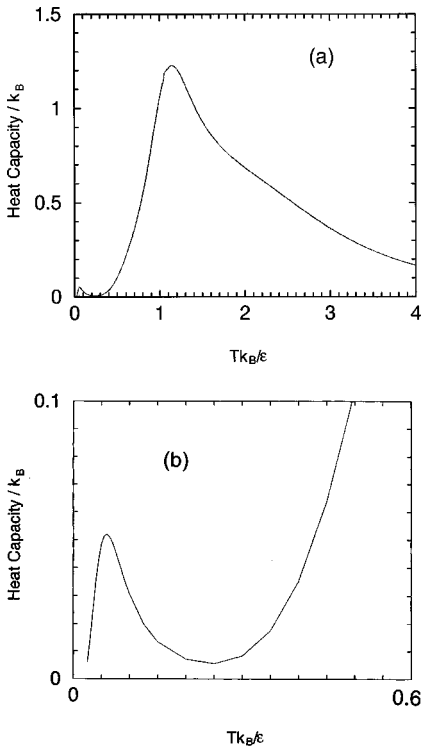


FIG. 4. Heat capacity calculated from a multicanonical Monte Carlo simulation in different temperature regions. Two peaks are visible, one corresponding to the collapsing transition from a denatured state and the other corresponding to the transition between states I and II. For a reduced temperature below 0.05, state I is more stable thermodynamically but cannot be reached easily kinetically (plot b).

### D. Thermodynamics

A multicanonical simulation uses a multicanonical weight to produce an almost flat multicanonical distribution independent of temperature. To calculate the temperature-dependent thermodynamic quantities based on a Boltzmann distribution, reweighting was performed for each given temperature in an implementation of similar technique described by Okamoto and Hansmann [15].

The heat capacity plot presented in Fig. 4 has two peaks. The large peak is located at a reduced temperature $\overline{T}=1.15$, above which the polymer displays an unfolded, coil state. The radius of gyration for a compact cubic configuration is 2. We observed from a radius of gyration measurement that below $\overline{T}\approx 1$ the 27 mer adopts compact conformations with a radius of gyration of 2. Figure 5 shows the structural overlapping parameters as a function of the temperature. The stable conformations in the $\overline{T}=0.5$ region are very close to the native structure, as represented by the dashed curve that has a value of 0.8 in this region. The solid curve, representing the overlap between the conformations

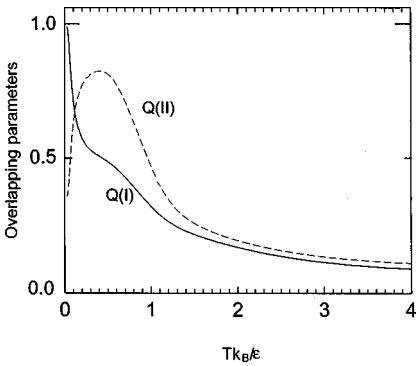


FIG. 5. The average overlapping parameters as a function of temperature. $Q(\mathrm{I})$ and $Q(\mathrm{II})$ represent the structural overlap with the ground state and excited state, respectively. The transition between states I and II at a reduced temperature of 0.05 is clearly visible in this figure.

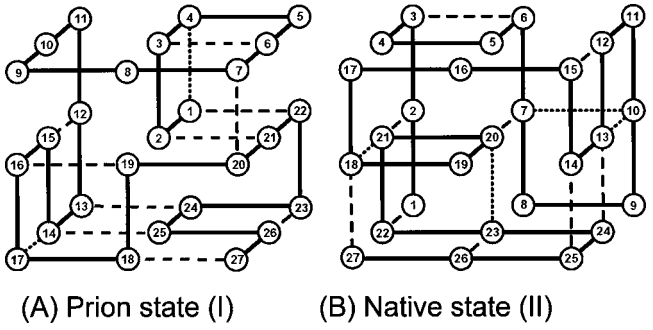


FIG. 6. The two native states of the prionlike sequence. Also shown are the similar-local bonds (long dashes) and the different-nonlocal bonds (short dashes). (a) The prion state, I. (b) The native state, II.

with the ground state, has a typical value of 0.4–0.5 in this region. Due to the definition of $Q$ and the fact that the two low-energy states share 10 common bonds out of the total 28, the overlapping parameter $Q[\mathrm{I}]$ would descend to an ideal minimum of 0.36 near structure II. This value represents the residual overlapping between structures I and II, and the actual conformations in the vicinity of $\overline{T}=0.5$ are similar to state II, hence has a $Q[\mathrm{I}]$ somewhat higher than 0.36.

The low-temperature peak in the heat capacity, as further displayed in Fig. 4(b) is not related to a change in the radius of gyration. As the temperature approaches zero the system attempts to find the global minimum energy state. As shown in Fig. 5, the average overlapping parameter $Q[\mathrm{I}]$ undergoes a rapid increase crossing the heat capacity peak at $\overline{T}=0.05$, whereas $Q[\mathrm{II}]$ decreases to a residual value between the two structure, I and II. From a thermodynamic perspective, there exist two stages of transition in this system. The collapsing transition is located at $\overline{T}=0.5$ and the stable state below this temperature is the excited state, II. In the region below $\overline{T}=0.05$, there is a structural transition between the state-II dominating conformations to the state-I dominating conformations.

### E. Folding time

The folding simulations mentioned in Sec. III A were conducted at a reduced temperature $\overline{T}=0.04$, where state I is considered more stable than II. However, due to the wider folding funnel allowed to the native state, II, a large percentage of the folding events reaches the native state.

We have estimated the MFPTs, directly from the folding trajectories to one of the states, either the native or the prion state. Table I lists the average folding time for various folding events. The folding from a denatured structure to the prion and native states, I and II, occurs rather quickly. These times are calculated based on the first passaging time and do not account for multiple unfolding/refolding events during the simulation. This can be compared with the previous results which suggest that the folding times for one of the two low-energy states should be much longer than the other in a kinetically partitioned landscape [12]. Our results are based on the folding trajectory not encountering the kinetic trap of the other low-energy state. If we include the time spent in the other energy minimum, then we have to take into account the folding time and the probability of the transition events between states I and II. When this is done, the folding times to state I would be much longer.

The folding times for the transition events are presented for only those that were able to make the transition in the limited simulation time. These transition times vary greatly and depend on the length of time spent in the respective energy minima. Thus, the transition times listed in Table I are not representative of the mean unfolding/refolding times between energy minima as we terminate the simulations at the $10^9$th MC step. Nevertheless, an examination of the crossover times listed in Table I demonstrates the existence of kinetic partitioning between the two states since the mean transition times are at least twice as long as the MFPTs.

### F. Bonding type

The structures that this sequence adopts are not designed to have any particular properties; this provides an opportunity to study the structural features of a "naturally" occurring lattice prion model. The two states for the sequence are shown in Fig. 6, and the energies for states I and II are $-78.596\epsilon$ and $-78.413\epsilon$, respectively. This is an energy difference of $0.183\epsilon$, while the energy gap between state II and the next-lowest-energy cube is $2.541\epsilon$.

To analyze the nature of the bonding, it is constructive to categorize the types of bonds as being local vs nonlocal. Local bonds are defined as bonds that form between the $i$th and $i$th$+3$ monomers, and the rest are considered nonlocal. This type of distinction was previously considered very important in understanding the folding nature of proteins [16].

Another method of analyzing bonding effects will be to categorize similar bonds that occur in both native structures. Distinguishing between the similar and different bonds will be important in the discussion of prion structures, because different bonds determine the difference of the two struc-

TABLE II. Bonding types for the prionlike sequence. Shown are the similar-local (SL), similar-nonlocal (SNL), different-local (DL), and different-nonlocal (DNL) bonds, for states I and II.

| | SL | SNL | DL (I) | DL (II) | DNL (I) | DNL (II) |
|---|---|---|---|---|---|---|
| No. Bonds | 4 | 6 | 2 | 4 | 16 | 14 |
| Average energy | −3.11 | −3.57 | −1.65 | −2.69 | −2.59 | −2.41 |
| Stand. dev. | 0.70 | 0.97 | 0.55 | 0.52 | 0.53 | 1.08 |

tures. In Fig. 6, the similar-nonlocal and different-local bonds are shown by long-dashed and short-dashed lines.

Table II lists the number of bonds of a particular type, the average bond strength, and the standard deviations in the average for each class of bonds. Both the similar-local and similar-nonlocal bonds have average interaction strengths that are much stronger than the average, which is preset by the mean of the Gaussian to $-2.0\epsilon$. These similar bonds play a significant role in the observed good folding properties of the sequence as we know that dominant local and nonlocal contacts produce faster folding sequences. It also appears that the similar-nonlocal bonds are much stronger than the different-nonlocal contacts, guiding the folding process through the folding funnels.

The different contacts kinetically partition the landscape of the sequence. The different-nonlocal contacts appear only to be slightly stronger than the average and are similar in value between the two native states, however state II has a much wider variation in the bond strengths as seen in the large standard deviation. This variation in the different-nonlocal bonds is important in the kinetic partitioning and characteristically separates the two structures.

The different-local contacts present a much different picture, as the variation in the average energy is large. In the good folding native state, II, the bond strengths are above average and there are more of them in this structure. This is fully consistent with the conclusion that dominant local contacts generate the kinetic partitioning in prions [12]. An interesting observation is that a large number of different-local contacts are not needed, and that these contacts do not have to be excessively strong.

## IV. CONCLUDING REMARKS

Using the simplified 27 mer lattice model, we are able to sort through the possible sequences and determine which of them exhibits prionlike behavior. Even at this most basic level of complexity, we observed sequences that mimic the properties of real prions with remarkable similarity. The results that prionlike protein landscape with a double energy minima is rare but do exist in a 27 mer model, provide a clue to identify the possibility of finding a prionlike structure in nature.

We present a detailed study of a prionlike sequence that helps us to understand the structure of a prion protein that has a preferred native state kinetically partitioned from its ground state. This property, however, is not inherent in all double energy minimum sequences, as most of them simply contain native structures similar to each other. The direct MFPTs to each state of our prionlike model are approximately equal. An observed asymmetry in the ability to cross between the two native states suggests that the landscape of these sequences is broken into two separate funnels.

Borg *et al.* [17] have recently suggested a more involved lattice model that also demonstrates the partitioning of the energy landscape. It will be interesting to investigate the infection scenario between the prion state and the native state, by examining the interaction between multiple copies of lattice proteins. Indeed, this has been discussed recently in terms of a two-dimensional lattice model [18].

## ACKNOWLEDGMENT

Financial support for this work was provided by the Natural Science and Engineering Research Council of Canada.

[1] S. B. Prusiner, Science **252**, 1515 (1991).
[2] N. Stahl, M. A. Baldwin, D. B. Teplow, L. Hood, B. W. Gibson, A. L. Burlingame, and S. B. Prusiner, Biochemistry **32**, 1991 (1993).
[3] G. C. Telling, P. Parchi, S. J. DeArmond, P. Cortelli, P. Montagna, R. Gabizon, J. Mastrianni, E. Lugaresi, P. Gambetti, and S. B. Prusiner, Science **274**, 2079 (1996).
[4] F. E. Cohen and S. B. Prusiner, Annu. Rev. Biochem. **67**, 793 (1998).
[5] S. B. Prusiner, D. Groth, A. Serban, N. Stahl, and R. Gabizon, Proc. Natl. Acad. Sci. U.S.A. **90**, 2793 (1993).
[6] G. S. Jackson, L. L. P. Hosszu, A. Power, A. F. Hill, J. Kenney, H. Saibil, C. J. Craven, J. P. Waltho, A. R. Clarke, and J. Collinge, Science **283**, 1935 (1999).
[7] A. Šali, E. I. Shakhnovich, and M. Karplus, Nature (London) **369**, 248 (1994).
[8] A. Šali, E. I. Shakhnovich, and M. Karplus, J. Mol. Biol. **235**, 1614 (1994).
[9] E. I. Shakhnovich, Curr. Opin. Struct. Biol. **7**, 29 (1997).
[10] H. S. Chan and K. A. Dill, Phys. Today **46**(2), 24 (1993).
[11] H. Li, C. Tang, and N. Wingreen, Phys. Rev. Lett. **79**, 765 (1997).
[12] V. I. Abkevich, A. M. Gutin, and E. I. Shakhnovich, Proteins **31**, 335 (1998).
[13] P. G. Wolynes, J. N. Onuchic, and D. Thirumalai, Science **267**, 1619 (1995).
[14] L. L. P. Hosszu, N. J. Baxter, G. S. Jackson, A. Power, A. R. Clarke, J. P. Waltho, C. J. Craven, and J. Collinge, Nat. Struct. Biol. **6**, 740 (1999).

[15] Y. Okamoto and U. H. E. Hansmann, J. Phys. Chem. **99**, 11 276 (1995).

[16] V. I. Abkevich, A. M. Gutin, and E. I. Shakhnovich, J. Mol. Biol. **252**, 460 (1995).

[17] J. Borg, M. H. Jensen, K. Sneppen, and G. Tiana, Phys. Rev. Lett. **86**, 1031 (2001).

[18] P. M. Harrison, H. S. Chan, S. B. Prusiner, and F. E. Cohen, Protein Sci. **10**, 819 (2001).